Journal of
Nanoscience and Nanotechnology
Vol. 11, 3911–3915, 2011

RESEARCH ARTICLE

Degradation and Failure of Field Emitting Carbon Nanotube Arrays

D. Roy Mahapatra[1,*], N. Sinha[2], and R. V. N. Melnik[3]

[1] Department of Aerospace Engineering, Indian Institute of Science, Bangalore 560012, India
[2] Department of Mechanical Engineering, Massachusetts Institute of Technology, Cambridge, MA, 02139, USA
[3] M^2 NeT Lab, Wilfrid Laurier University, Waterloo, ON, N2L3C5, Canada

It has been observed experimentally that the collective field emission from an array of Carbon Nanotubes (CNTs) exhibits fluctuation and degradation, and produces thermal spikes, resulting in electro-mechanical fatigue and failure of CNTs. Based on a new coupled multiphysics model incorporating the electron–phonon transport and thermo-electrically activated breakdown, a novel method for estimating accurately the lifetime of CNT arrays has been developed in this paper. The main results are discussed for CNT arrays during the field emission process. It is shown that the time-to-failure of CNT arrays increases with the decrease in the angle of tip orientation. This observation has important ramifications for such areas as biomedical X-ray devices using patterned films of CNTs.

Keywords: Field Emission, Carbon Nanotube, Defect, Fatigue, Electrical Breakdown, Phonon, Multiscale Model.

1. INTRODUCTION

Arrays of Carbon Nanotubes (CNTs) grown on various types of substrate have shown promise as nano-structured cathode with possible applications in field emission devices, nano-scale imaging and X-ray sources.[1,2] However, in a patterned array of CNT field emitters one observes fluctuation of collective field emission current, often with large spikes, and failure of CNTs.[3,4] Several studies have been reported, which shed light on various different possible mechanisms such as electrodynamic force activated failure in isolated CNT,[4] electron–phonon interaction effect causing degradation in emission current,[5] electrical breakdown[6,7] and thermal degradation of isolated CNTs.[8–10] Such degradation mechanisms have their origin in (i) the electro-mechanical force field leading to the deformation of CNTs and (ii) coupled electron–phonon transport, thereby, producing temperature spikes under high electric field, and (iii) thermo-mechanically activated fracture of the tubular grapehene sheet. The temperature of certin regions of the array can be high enough to activate structural breakdown of CNT and sometimes even the substrate. In addition to such sudden failure, structural defects in CNT may grow even at moderate temperature. These defects result can affect the field emission current. In an array of CNTs, the overall failure process is however not predictable by extrapolating the results based on single CNT experiments. Non-local interaction in an array, segment-by-segment failure of CNTs and statistics of the array need to be considered. Overall, solving this problem of array of CNTs would make the design of patterned field emitting films possible.

In biomedical X-ray devices and many other applications, any fluctuation or degradation of emission performance and occurrence of any thermal spikes (leading to failure of CNTs) are undesirable and hence need to be minimized. In biomedical X-ray imaging and delivery systems, it is very important to have (i) cathodes with reliable lifetime and (ii) precise control of electron beams over multiple spatio-temporal scales. Therefore, it is important to develop physics based models, incorporating these factors, in order to predict failure of CNTs. In view of the coupled nature of electrical and thermal degradation, in this paper, we extend the previously developed model[11,12] to include the details of the electron–phonon transport and the electrical breakdown. Further we employ a kinetic model of fracture based on the Maxwell-Boltzmann distribution of thermal vibration of the toms under electric field and ballistic transport of electrons. Finally, the time-to-failure for the CNTs are estimated with the help of non-equilibrium strain field in the CNTs obtained from the previously developed coupled model.[11,12]

*Author to whom correspondence should be addressed.

2. METHOD

In the field emission problem under consideration, the CNTs, as grown on a substrate, can be in the form of random or patterned array. We call this system as CNT film. Assuming that lattice defects exist at various sites, we model such sites by introducing a random distribution of defects over the CNT array. An activation energy of $\triangle$ is assumed. For CNTs with small bandgaps, which is much smaller than activation energy for the Stone-Wales defect ($\sim$10 eV), it is reasonable to assume that life of CNTs would be quite long unless there are severe stress components of particular forms which enhance fracture under electric field. Whereas, it is more probable that large temperature gradients could be large enough to cross over the value of $\triangle$. It was reported in Ref. [13] that $\sigma - \pi^*$ transition energy in some CNTs can have energies comparable to the defect activation energy $\triangle$, which means that field emission involving such transition could lead to weakening of bonds. Again, it may be noted that vibration of such bonds (phonons) may have strong resonance at certain temperatures and electron densities. The ballistic transport of electrons from the tips of the CNTs produces large thermal gradients, and it has been postulated that electrical breakdown may occur at a distinct temperature $T_b \sim 900$ K. Assuming that such breakdown temperature is known for a particular type of CNT, we assume that the total electron density (n) is proportional to the number of carbon atoms (N) of CNTs in the unit representative cell of the film until physical breaking of bonds, that is nN. Here, a unit cell is a representation of a specified number of as grown CNTs confined by the cathode substrate below and the anode surface from above with free space in between.[11, 12] Accounting for thermally activated defect, the evolved electron density is expressed as

$$n = \int_0^t n_0 \frac{2\pi}{\tau_A} \exp\left(\frac{-\triangle}{k_B T}\right) dt, \quad T_c < T \leq T_b \tag{1}$$

$$n_{t_{i+1}} = n_{t_i} \frac{2\pi}{\tau_A} \exp\left(\frac{-\triangle}{k_B T}\right)(t_{i+1} - t_i), \quad T > T_b \tag{2}$$

and we perform time stepping until $n_{t_{i+1}} \leq 0$, which corresponds to either complete fracture or complete Coulomb blockade. Here n_0 is the surface electron density corresponding to Fermi level energy, τ_A is the relaxation time constant (in the range of 10^8–10^{18} s^{-1}), k_B is the Boltzmann's constant and T_c is a critical temperature above which the coupling between the thermal transport and the electron transport is strong such that defects are activated. Such temperature rise could occur following the transients with frequencies satisfying the condition

$$\omega > n_0 \left(\frac{\pi d_t^{(p)} e E_{Z'} + b_2}{2E' A_0}\right)\sqrt{\frac{E'}{\rho}} \tag{3}$$

where ω is the circular frequency, d_t is the diameter of the pth CNT, e is the positive electronic charge, $E_{z'}$ is the background electric field, b_2 is the energy due to Coulomb interaction, E' is the effective modulus of elasticity of CNTs under consideration, A_0 is the effective cross-sectional area of CNTs due to orbital size over the ring and ρ is the mass per unit length of CNT. In order to introduce structural degradation and fracture induced failure process, we adopt the inflection point approach, where in the light of Zhurkov's model, the lifetime τ_i of a strained ith mode crack front behind a C–C bond in a CNT is given by Ref. [14]

$$\tau_i = \tau_0 \exp\left(\frac{U_0 - \bar{U}_i}{k_B T}\right), \tag{4}$$

where U_0 is the bond dissociation energy and $\bar{U}_i$ is the zero temperature strain energy of the C–C bond, such that $\triangle\bar{U} = U_0 - \bar{U}_i$ is the energy barrier against the fracture across the C–C bond at the crack front. According to the inflection point approach, the assumption is that the bond dislocation starts at the peak value of the tensile stress and U_0 is the corresponding dislocation energy. Equation (4) accounts for the fact that dislocation is the combined effect of thermal motion of the atom and the tensile stress, which together lowers the energy barrier. Again, the thermal motion has strong correlation with electron emission and transition of orbital electrons as discussed in context of Eqs. (1) and (2).

From the developed multiscale model of electrodynamic stretching of the CNTs, coupled with heat transport and electron density calculations, we estimate the tensile strains along the CNTs (treated as one-dimensional elastic elements made of tubular segments). Under the assumption of small strain and small curvature, the longitudinal strain ϵ_{zz} (including thermal strain) and stress σ_{zz} can be written as, respectively,[12]

$$\epsilon_{zz} = \frac{\partial u_{z'0}^{(m)}}{\partial z'} - r^{(m)} \frac{\partial^2 u_{x'}^{(m)}}{\partial z'^2} + \alpha\triangle T(z'), \qquad \sigma_{zz} = E'\epsilon_{zz}, \tag{5}$$

where $\triangle T(z') = T(z') - T_0$ is the difference between the absolute temperature (T) during field emission and a reference temperature (T_0), and α is the effective coefficient of thermal expansion (longitudinal). We approximate the strain energies of the bonds as

$$\bar{U}_i = b_i \epsilon_{zz}^2 \tag{6}$$

where b_i are constants fitted from the bond energy versus tensile strain curves.[15] In the following numerical simulations, we use the values of b_i from Ref. [14] which is for (18, 0) zigzag type nanotube. Strains and current densities are calculated using the same geometry of the CNTs, i.e., (18, 0) configuration. There are 18 bonds to fail for complete fracture in the circumferential mode, that is $i = 1, \ldots, 18$. Assuming that we have single mode fracture, the time-to-failure (τ) of an intact CNT is given by

$$\tau = \sum_i \tau_i = \sum_i \tau_0 \exp\left(\frac{U_0 - b_i \epsilon_{zz}^2}{k_B T}\right)^2 \tag{7}$$

where the strain at the inflection point is estimated to be 19% (see Ref. [16]) and the corresponding bond dissociation energy U_0 is 1.84×10^{-19} J.

3. RESULTS AND DISCUSSIONS

The CNT film considered for the analysis here consists of randomly oriented CNTs. The film surface area (projected on the anode) is 49.93 mm^2 and the average height of the film (based on randomly distributed CNTs) is 10–14 μm. With the basic modeling approach, numerically simulated I–V curves for various types of CNTs have been found to be in close agreement with the experimental curves.[11] We use the following sample configuration: average height of CNTs $h_0 = 12$ μm and uniform spacing $d_1 = 2$ μm at the substrate contact regions. A random initial height distribution with range $h = h_0 \pm 2$ μm and random orientation angle θ at the nodes are given. The random orientation effect is parameterized in terms of the initially assigned tip deflection (denoted by h/m', $m' > 1$). The gap (d) between the electrodes is maintained at 34.7 μm. Several computational runs were performed and the output data were averaged out at each sampling time step.

Figure 1 shows field emission current histories for the CNT thin film with different initial tip orientations. It is seen from the figure that for small tip orientations (such as h/25 in the present case), the current rises in steps. However, as the tip orientation or the initial state of deflection is increased, the average current reduces, until, h/m' becomes large enough so that the electrodynamic interaction among CNTs produces a sudden pull in the deflected CNTs (see the CNT marked "A" in Fig. 2) leading to transients in the output current. The results in Figure 2 are in agreement with a study reported in literature.[17]

The results of time-to-failure for the CNT array system with various tip orientations and under various applied bias fields are shown in Figure 3. As evident from Figure 3, the time-to-failure of CNT arrays for large angle of orientation of the tip (h/15) decreases as the applied bias field is increased. This is due to large bending and stretching of these CNTs during field emission, leading to growth of defect and fracture. Our numerical results suggest that the time-to-failure of CNT arrays increases with the decrease in the angle of tip orientation. When the tip orientation is further decreased, the time-to-failure becomes approximately constant under different applied bias field regimes. This is an important result, which gives important insight towards understanding the degradation and failure mechanism of CNTs and their lifetime estimation in context of field emission device.

Next, the maximum current and the average current for various diameters and bias voltages were computed using statistical analysis of the simulated data. The corresponding results are plotted in Figure 4. Following observations can be drawn from this figure: (i) as the applied bias field is increased, the output current is increased (which is

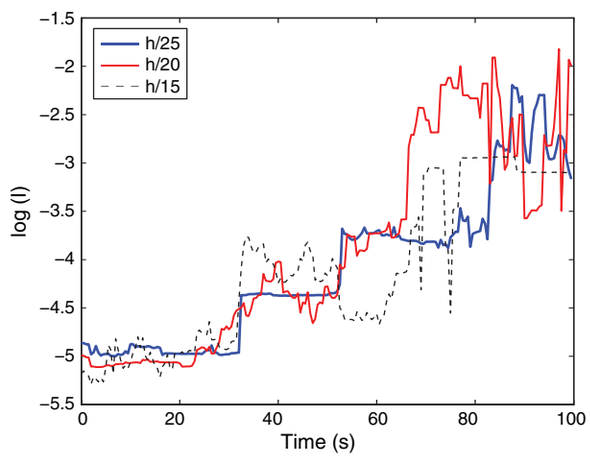

Fig. 1. Field emission current history at initial stage showing step-wise rise in the current for small tip orientations (h/25) and transients in the current for larger tip orientations (h/20, h/15).

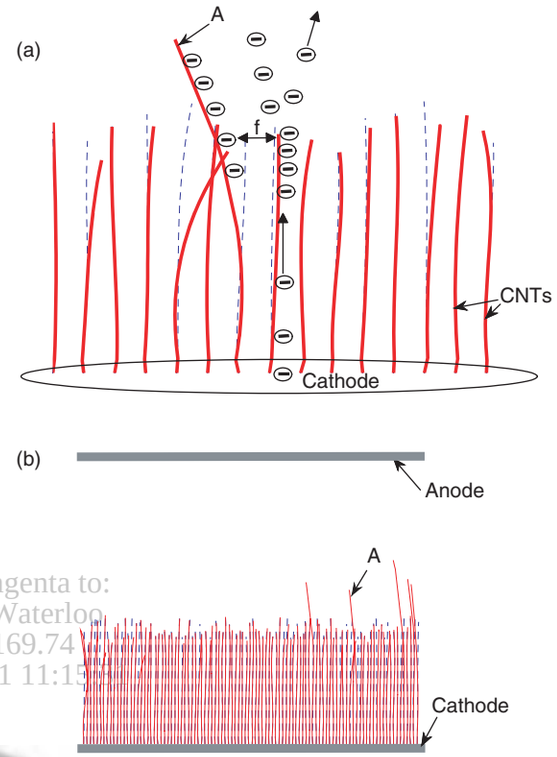

Fig. 2. (a) Array of 100 CNTs (non-uniform height distribution with variation $\pm h/20$) modeled as one-dimensional elastic members and indicated by the solid lines, showing the deformed configuration of the tubes obtained by numerical simulation. Intial state shown by dashed lines. Deformed configuration snap taken at $t = 100$ s of field emission. (b) Enlarged view (not to the scale) of the region near the pulled up CNT (marked as "A"). The initial shape is shown by dashed line and the deflected configuration at $t = 100$ s is shown by the solid line. f indicates the force due to combined effect of Coulombic interaction, and electrodynamic force due to moving electrons, including the dynamics of CNTs.

RESEARCH ARTICLE

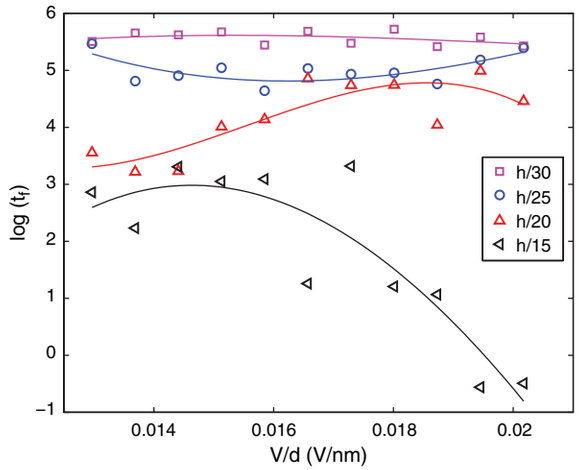

Fig. 3. Time-to-failure for the CNT array system with various tip orientations and under various applied bias fields.

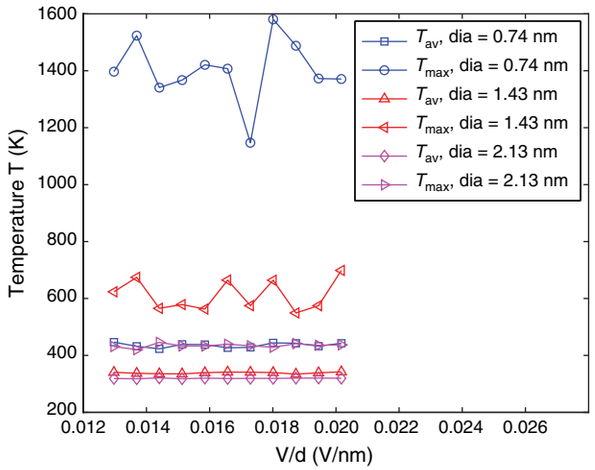

Fig. 5. Average temperature (T_{av}) and maximum temperature (T_{max}) over time versus applied bias field for CNT arrays with various diameters of CNTs and for initial distribution of tip orientations of $h/20$.

physically consistent); and (ii) the output current is higher for smaller diameter CNTs ($d_t = 0.74$ nm). This result validates the experimental studies in literature, reporting that sharp tips produce more current.[18, 19] However, at lower diameter values, there is a large fluctuation of the field emission current. An almost linear I versus V/d behavior can be observed for higher diameter values in Figure 4.

In Figure 5, we plot the maximum temperature and average temperature for various bias voltages and different diameters. As evident from Figure 5, the variation in average temperature is almost independent of the applied bias field. However, large fluctuation in maximum temperature (1180 K to 1600 K) is observed for small diameter ($d_t = 0.74$ nm) CNTs. As this temperature range is larger than the breakdown temperature T_c (generally > 900 K), there may be degradation of CNTs resulting in a proportional decrease in the electron density at a rate $n\omega_c \exp(-\Delta_c/(k_B T_c))$, where ω_c is the highest frequency in the spectrum of the temperature spike and $\Delta\omega_c \sim 3$–4 eV.[8]

Based on the simulations performed, the stress in the CNTs at various applied bias fields and varying diameters were estimated using Eq. (5). The results are shown in Figure 6. For $d_t = 0.74$ nm, the h/d_t ratio is the highest among the three cases. Therefore, the stress in the CNTs for this case is larger than in the other two cases. The maximum stress for $d_t = 0.74$ nm varies between 6 to 22 GPa, while it is low and almost constant for $d_t = 2.13$ nm. It can be concluded that although small diameter (sharp tip) CNTs are good for producing more current, there is less stress in CNTs with large diameter. However, the maximum stress in all the cases is well below the fracture stress (65–93 GPa).[16]

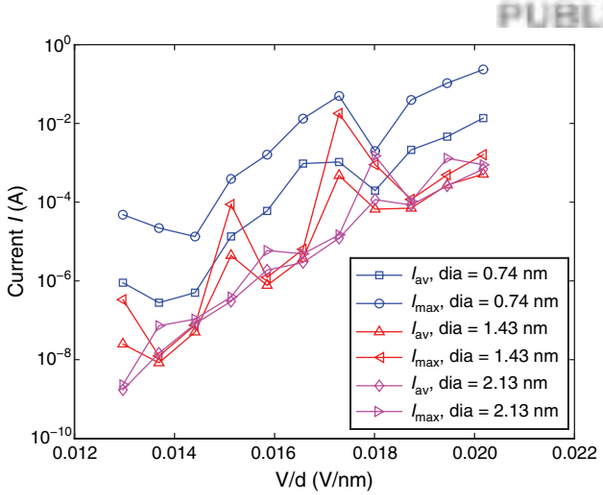

Fig. 4. Average current (I_{av}) and maximum current (I_{max}) over time versus applied bias field for CNT arrays with various diameters of CNTs and for initial distribution of tip orientations of $h/20$.

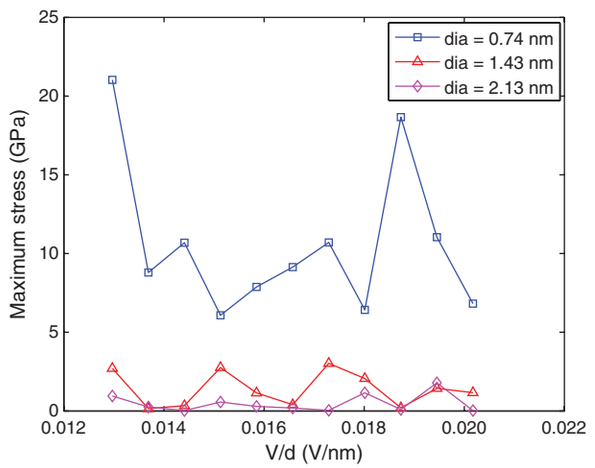

Fig. 6. Maximum stress in the CNT array versus applied bias field for various diameters of CNTs.

4. CONCLUSIONS

In this paper, we have developed a method to analyze collective field emission and resulting degradation and failure of CNTs in a thin film. It has been shown how stress and strain in a CNT array during field emission can be estimated using the proposed methodology. Consequently, the lifetime of CNTs can be predicted using the concept of bond strain energy concentration and the classical kinetic concept of bond fracture.

References and Notes

1. Z. W. Pan, F. C. K. Au, H. L. Lai, W. Y. Zhou, L. F. Sun, Z. Q. Liu, D. S. Tang, C. S. Lee, S. T. Lee, and S. S. Xie, *J. Phys. Chem. B* 105, 1519 **(2001)**.
2. N. De Jonge and J.-M. Bonard, *Royal Soc. London A* 362, 2239 **(2004)**.
3. L. Nilsson, O. Groening, P. Groening, and L. Schlapbach, *Appl. Phys. Lett.* 79, 1036 **(2001)**.
4. J.-M. Bonard and C. Klinke, *Phys. Rev. B* 67, 115406 **(2003)**.
5. M. Steiner, H. Qian, A. Hartschuh, and A. J. Meixner, *Nano Lett.* 7, 2239 **(2007)**.
6. P. G. Collins, M. Hersam, M. Arnold, R. Martel, and Ph. Avouris, *Phys. Rev. Lett.* 86, 3128 **(2001)**.
7. R. V. Seidel, A. P. Graham, B. Rajasekharan, E. Unger, M. Liebau, G. S. Duesberg, F. Kreupl, and W. Hoenlein, *J. Appl. Phys.* 96, 6694 **(2004)**.
8. H.-Y. Chiu, V. V. Deshpande, H. W. Ch. Postma, C. N. Lau, C. Miko, L. Forro, and M. Bockrath, *Phys. Rev. Lett.* 95, 226101 **(2005)**.
9. N. Y. Huang, J. C. She, J. Chen, S. Z. Deng, N. S. Xu, H. Bishop, S. E. Huq, L. Wang, D. Y. Zhong, E. G. Wang, and D. M. Chen, *Phys. Rev. Lett.* 93, 075501 **(2004)**.
10. W. Wei, W. Wei, Y. Liu, Y. Wei, K. Jiang, L.-M. Peng, and S. Fan, *Nano Lett.* 7, 64 **(2007)**.
11. N. Sinha, D. Roy Mahapatra, J. T. W. Yeow, R. V. N. Melnik, and D. A. Jaffray, *J. Comput. Theor. Nanosci.* 4, 535 **(2007)**.
12. N. Sinha, D. Roy Mahapatra, Y. Sun, J. T. W. Yeow, R. V. N. Melnik, and D. A. Jaffray, *Nanotechnology* 19, 025701 **(2008)**.
13. M. S. Dresselhaus, G. Dresselhaus, and P. C. Eklund, Science of Fullerenes and Carbon Nanotubes, Academic Press, New York **(1996)**.
14. T. Xiao, Y. Ren, and K. Liao, *Nano Lett.* 4, 1139 **(2004)**.
15. T. Xiao and K. Liao, *Phys. Rev. B* 66, 153407 **(2002)**.
16. T. Belytschko, S. P. Xiao, G. C. Schatz, and R. S. Ruoff, *Phys. Rev. B* 65, 235430 **(2002)**.
17. A. I. Zhbanov and O. E. Glukhova, *IEEE Proc. 14th Int. Vacuum Microelectronic Conf.* 63 **(2001)**.
18. J.-M. Bonard, F. Maier, T. Stockli, A. Chatelain, W. A. De Heer, J.-P. Salvetat, and L. Forro, *Ultramicroscopy* 73, 7 **(1998)**.
19. J.-M. Bonard, J.-P. Salvetat, T. Stockli, W. A. De Heer, L. Forro, and A. Chatelain, *Appl. Phys. Lett.* 73, 918 **(1998)**.

Received: 18 June 2010. Accepted: 7 July 2010.